Chemical Science

ROYAL SOCIETY OF CHEMISTRY

EDGE ARTICLE

View Article Online
View Journal | View Issue

Cite this: *Chem. Sci.*, 2023, **14**, 11441

All publication charges for this article have been paid for by the Royal Society of Chemistry

Received 2nd July 2023
Accepted 30th September 2023

DOI: 10.1039/d3sc03364c

rsc.li/chemical-science

Unlimiting ionic conduction: manipulating hydration dynamics through vibrational strong coupling of water†

Tomohiro Fukushima, * Soushi Yoshimitsu and Kei Murakoshi *

The energy states of molecules and the vacuum electromagnetic field can be hybridized to form a strong coupling state. In particular, it has been demonstrated that vibrational strong coupling can be used to modify the chemical dynamics of molecules. Here, we propose that ion dynamics can be altered through modifications of the dynamic hydration structure in a cavity vacuum field. We investigated the effect of different electrolyte species on ionic conductivity. Infrared spectroscopy of aqueous electrolyte solutions within the cavity confirmed the formation of vibrational ultrastrong coupling of water molecules, even in the presence of electrolytes. Interestingly, we observed significant enhancements in ionic conductivity, for specific alkali cations, particularly those classified as structure-breaking cations. These enhancements cannot be explained within the current theoretical framework for liquid electrolytes. Our analysis suggests that the vibrational strong coupling modifies the local dielectric friction experienced by hydrated ions. In addition, we propose the enthalpic and entropic modification of ionic conductivity through the systematic investigation of the hydration properties of different electrolytes. This study unveils the potential role of polaritons for exploring uncharted spaces in the design of materials with enhanced ionic conduction. Harnessing the unique properties of strong coupling and its influence on hydration dynamics could lead to the development of novel electrolytes and advancements in the field of ionic conduction.

Introduction

Various inorganic and organic materials have been used as ionic conductors,[1–4] which are important in energy technologies, such as electrolyzers, batteries, and sensors. In particular, water plays an important role in ionic conduction.[5–9] Charge transport in electrochemical energy-conversion systems involves the diffusion and migration of hydrated ions in aqueous electrolyte solutions. Ion transport is influenced by the hydration properties of the ion species.[9–13] In general, ion conduction in aqueous electrolyte solutions can be classified as either proton (H^+) conductivity or classical ion transfer. The former mechanism is characterized by the quantum transfer of H^+ ions and the reorientation of water molecules.[14–19] It is commonly known as the Grotthuss mechanism.[20,21] In the second mechanism, ion migration is governed by the competition between migration effects and friction. This is also known as the vehicle mechanism.[22] Friction arises from the viscosity and dielectric environment of the electrolyte solution.[23] Therefore, a molecular-level understanding of intermolecular interactions and dynamic hydration behavior is crucial. However, currently, there are no effective methods to control hydration in ion dynamics which limit the transport phenomenon.

Recently, an emerging field of research known as polaritonic chemistry has been proposed, which explores the interaction between light and matter, even in the absence of an external light illumination.[24–27] In this field, the electromagnetic fluctuations of the vacuum field in an optical resonator can interact with molecules inside the resonator to create a state of coherent coupling. When molecules are placed in a micrometer-scale cavity, physicochemical phenomena can be modified.[28–30] The modification under vibrational strong coupling can be emphasized especially for the coupling with solvents because of the large number of molecules.[31] Notably, water has been shown to exhibit an ultrastrong coupling regime,[32–38] allowing for modifications in its physicochemical properties. This phenomenon has been demonstrated in various contexts, including the modulation of hydrogen-bonding networks,[32] the manipulation of enzymatic activity,[33,34] the modification of DNA replication[35] and the folding of DNA origami,[36] and the selective crystallization of metal–organic frameworks.[37] In our previous work, we discovered a more than tenfold enhancement in the H^+ conductivity of aqueous solutions.[38] We hypothesized that

Department of Chemistry, Faculty of Science, Hokkaido University, Sapporo, Hokkaido, 060-0810, Japan. E-mail: tfuku@sci.hokudai.ac.jp; kei@sci.hokudai.ac.jp

† Electronic supplementary information (ESI) available. See DOI: https://doi.org/10.1039/d3sc03364c

water-molecule hydration could be modified through vibrational strong coupling.

Here, we reveal the effect of hydration on the ionic conductivity of cations and anions under vibrational strong coupling. We conducted a systematic study on alkali metal-halide solutions and observed an increase in the ionic conductivity as a result of the modified hydration under vibrational strong coupling. We propose a mechanism in which vibrational strong coupling modifies the hydration dynamics. Importantly, the nature of hydration influences ionic conductivity.

Results and discussion

Vibrational strong coupling of aqueous electrolytes

The formation of vibrational strong coupling states was confirmed using infrared (IR) transmission spectroscopy, and representative IR spectra are shown in Fig. 1a. When the cavity mode was matched to the O–H stretching frequency of water ($\omega_{st,OH} = 3400\ cm^{-1}$), the original absorption peak disappeared, and two distinct peaks corresponding to vibro-polaritonic states emerged. This phenomenon is consistent with previous reports on the vibrational strong coupling of water.[32–38] The anti-crossing behavior of the upper and lower polariton branches was evaluated, as shown in Fig. 1b. The frequency of the third-order cavity mode was adjusted by controlling the cavity thickness within the range of 2.8 to 4.0 μm. The third order of cavity mode was selected to avoid the resonance effect of the bending mode of water (1600 cm^{-1}). The cavity thickness was determined from the free spectral range of the cavity fringe (see ESI†).[24,28,29,32–38] We investigated electrolyte solutions of LiCl, NaCl, KCl, RbCl, CsCl, Me_4NCl, Et_4NCl, $^nPr_4NCl$, $^nBu_4NCl$, LiF, and LiBr. The quality factor of the fourth-order cavity mode varied between 22 and 25 in each independent experiment. Even in the presence of electrolyte, the observed anti-crossing behavior remained consistent. Consistent vibro-polaritonic behavior was observed for combinations of alkali cations, tetraalkylammonium cations, and halide anions. This is reasonable because the concentration of the electrolyte (0.01 M) was significantly lower than the concentration of water (55.5 M). The Rabi splitting frequency was estimated when the cavity mode was tuned to the O–H stretching frequency, resulting in a value of 760 cm^{-1}. This value is similar to that in reports on vibrational polaritons in pure water.[32–38] Under strong coupling conditions, the optical mode was confined within the cavity, enabling coherent interactions with the vibrational mode of water. Under these conditions, ω_R exceeded the sum of the photon loss rate of the cavity and the dephasing rate of the O–H stretching frequency of water molecules.[39,40] The photon loss rate of the cavity mode was estimated as 200 cm^{-1}. The homogeneous line width of the O–H stretching mode, which corresponds to the dephasing rate of the vibrational modes, was 120 cm^{-1}.[41] The relationships between the Rabi splitting energy, photon loss rate, and dephasing rate provide support for the clear formation of vibrational strong coupling states of water molecules in the cavity, even in the presence of an electrolyte. This system achieved particularly strong vibrational ultrastrong coupling, where $\omega_R/2\omega_{st,OH} = 0.11$, which is a benchmark for molecules coupled to vacuum fields.[42,43]

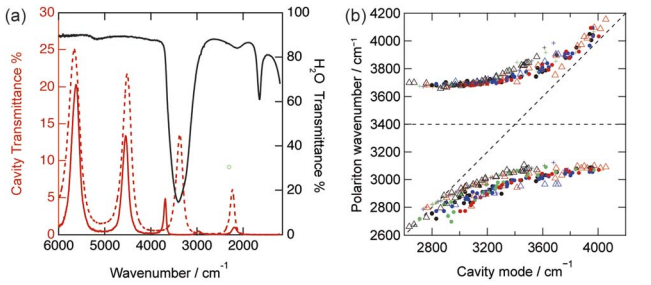

Fig. 1 (a) Representative IR transmission spectra of the air-filled cavity (red dotted line) and the water-filled cavity (red solid line). The cavity thickness of air-filled cavity was 4.5 μm. The cavity thickness of water-filled cavity was 3.7 μm. The black line represents IR transmission spectra of a 0.01 M KCl aqueous electrolyte. (b) Anti-crossing behavior of the upper and lower polariton peaks with a third-order cavity mode, where the typical cavity thickness varies between 2.8 and 4.0 μm, for: LiCl (black solid circles), NaCl (blue solid circles), KCl (green solid circles), RbCl (red solid circles), CsCl (purple solid circles), LiF (black open circles), LiBr (red open circles), Me_4NCl (black crosses), Et_4NCl (blue crosses), $^nPr_4NCl$ (green crosses), and $^nBu_4NCl$ (red crosses). The light line and O–H stretching frequencies are shown as dotted lines.

Modulation of ionic conductivity under vibrational strong coupling

We evaluated the modulation of ionic conductivity under vibrational ultrastrong coupling. Fig. 2a illustrates the dependence of ionic conductivity on the cation species in 0.01 M MCl aqueous electrolyte solutions (M = Li, Na, K, Rb, and Cs). The control experiments of bulk ionic conductivity have been conducted by using the same cell without the Au mirrors (see ESI†).[38] Notably, the modulation of the ionic conductivity depended on the cation species. For example, the bulk ionic conductivity of LiCl (0.11 S m^{-1}) was comparable to its ionic conductivity in the cavity (0.14 S m^{-1}). By contrast, the ionic conductivity of CsCl in the cavity (0.41 S m^{-1}) was three times higher than its bulk ionic conductivity (0.15 S m^{-1}). For all cations, the highest ionic conductivity was observed at a cavity thickness of approximately 3.3 μm, which corresponds to the

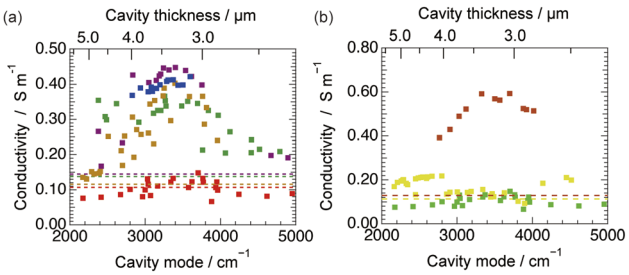

Fig. 2 Modulation of ionic conductivity by detuning the cavity mode. (a) Effect of the cation on the ionic conductivity, with data shown for 0.01 M LiCl (red), NaCl (green), KCl (brown), RbCl (blue), and CsCl (purple) aqueous electrolytes. (b) Effect of the anion on the ionic conductivity, with data shown for 0.01 M LiF (yellow), LiCl (green), and LiBr (brown) aqueous electrolyte.

coupling of the third-order cavity mode with the O–H stretching mode. This suggests that the coupling of the O–H stretching mode of water enhances the ionic conductivity.

We investigated the modulation of ionic conductivity by different anion species. We selected lithium as the cation species because we observed that it modulated the ionic conductivity very weakly under vibrational ultrastrong coupling. Fig. 2b illustrates the dependence of the ionic conductivity in 0.01 M LiX aqueous electrolyte solutions (X = F, Cl, and Br). The values for fluoride and chloride anions did not change appreciably under vibrational ultrastrong coupling. By contrast, the ionic conductivity of LiBr aqueous electrolyte solution in the cavity was three times higher than its bulk ionic conductivity. We also attempted to evaluate the ionic conductivity using LiI; however, the mirrors peeled off because of the corrosive nature of iodide on the Au surface, even when covered with SiO_2. The scattered data in ionic conductivity in this case may arise from the instability of the cell in the electrolyte solution. We assume the origin of the broad resonance might be originated from the micro-solvation environments. In summary, we demonstrated the independent modulation of cationic and anionic conductivity through vibrational coupling of ionic hydration.

Temperature dependence

The temperature dependence of the ionic conductivity was investigated under vibrational strong coupling, as shown in Fig. 3. The third order of the cavity mode was detuned to the O–H stretching mode by adjusting the cavity thickness to 3.3 μm. Temperature control was achieved using a custom-made cell. IR transmission spectra were obtained before and after the electrochemical measurements to confirm the coupling state (detailed experimental conditions are described in the ESI†). The validity of the results was confirmed by control experiments (Fig. S2†). Importantly, the temperature dependence was modulated under vibrational strong coupling. In particular, linear temperature dependence was observed for the CsCl aqueous electrolyte. Nonlinear dependence was observed for KCl and $HClO_4$. In most cases, linear Arrhenius behavior was observed. This is because a simple model with a defined diffusion constant can characterize the state of ionic conductivity. The nonlinear behavior might be due to the non-linearity in the local hydration around the ions depending on temperature. In addition, the apparent activation energies of CsCl aqueous electrolyte solution in the cavity were higher than its values in the bulk. We also investigated H^+ conductivity. However, modulation of the activation energy was not observed, despite the greatly enhanced conductivities. This suggests the contribution of a distinct mechanism to the activation process of ion conduction under vibrational strong coupling.[38]

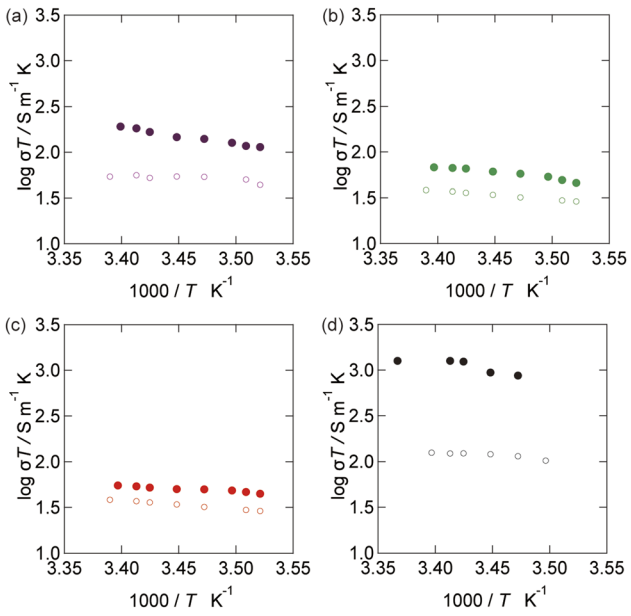

Fig. 3 Temperature dependence of ionic conductivities. (a) CsCl, (b) KCl, (c) LiCl, and (d) $HClO_4$. The solid circles represent the ionic conductivity in the cavity. The open circles represent the ionic conductivity in the cavity.

Effect of vibrational strong coupling on hydration

Historically, the transport of ions has been described using nonequilibrium statistical mechanics, such as the Debye–Hückel–Onsager–Falkenhagen theory. In this theory, ions are treated as Brownian particles in a continuum dielectric solvent, interacting through coulombic forces. Because ions are in continuous motion, the frictional force acting on them is proportional to their velocity.[13,44,45] Stokes law, which is derived from hydrodynamic theory and states that friction increases with increasing ionic radius, fails to accurately describe small alkali and halide ions.[13,46,47] The total friction, ζ_i, is described as the sum of the hydrodynamic friction, ζ^H, and dielectric friction, ζ^D, according to the following equation ($\zeta = \zeta^H + \zeta^D$). The hydrodynamic friction is proportional to the ion size and is given by Stokes law with slip boundary conditions ($\zeta^H = 4\pi\eta r_{ion}$), where r_{ion} is the Stokes radius of the ion and η is the solvent viscosity. In continuum treatments, the dielectric friction is usually characterized by a single relaxation time, ($\zeta^D = 3q_{ion}{}^2(\varepsilon_0 - \varepsilon_\infty)\tau_D/4r_{ion}{}^3\varepsilon_0{}^2$), where q_{ion} is the ion charge, ε_0 is the vacuum permittivity, ε_∞ is the high-frequency dielectric constant, and τ_D is the dielectric relaxation time.

In an attempt to explain the unique behavior of small ions in polar solvents, two models have been proposed that attribute different phenomena to the solvent response and solute or ion displacement. The first model, which is often referred to as the solvent-berg model, maintains a classical view of Stokes law but introduces an "effective" ionic radius that arises from solvation. In this model, solvent molecules are considered to be bound to the ion, and the radius of the solvated complex is equivalent to the Stokes radius. The other model is the dielectric-friction model, which has been developed over several decades by Born,[48] Fuoss,[49] Boyd,[44] and Zwanzig,[50,51] with a comprehensive theoretical framework established by Hubbard and Onsager.[52,53] This model aims to describe the dielectric response of the solvent when perturbed by the motion of an ion. As the ion moves away from its initial position, where the solvent is polarized according to the electrostatic field generated by the

ion, the solvent polarization does not immediately equilibrate with the new position of the ion. This leads to a relaxation process and subsequent dissipation of energy in the form of dielectric friction. The dielectric friction is inversely related to the ionic radius. As a result, the friction coefficient reaches a minimum value with increasing ionic radius in both models.

Fig. 4 illustrates the correlations between ionic conductivity and ionic radius in bulk and under vibrational strong coupling. The plot includes the ionic conductivity of electrolyte solutions with and without the cavity. We note that the slight increase in ionic conductivity can be attributed to the high transport number of the counter anion, Cl^-. Alkylammonium cations exhibited a linear relationship with the cation's ionic radius, r_{ion}. This behavior is consistent with Stokes' law, according to which the viscosity strongly influences ionic conductivity. The hydrodynamic friction ($\zeta^H = 4\pi\eta r_{ion}$) is minimally affected by vibrational strong coupling, indicating that the effect of water viscosity by vibrational strong coupling was negligible. Alkali cation species displayed an inflection in their ionic conduction with increasing ionic radius. We attribute this to the dynamic hydration process, which is described by the component in the relaxation time of dielectric friction ($\zeta^D = 3q_{ion}{}^2(\varepsilon_0 - \varepsilon_\infty)\tau_D/4r_{ion}{}^3\varepsilon_0{}^2$). Li ions are strongly hydrated by water molecules, leading to the formation of a structured network of hydrogen bonding between water molecules. By contrast, because of the low charge density of Cs ions, water molecules are weakly hydrated, resulting in unstable water networks. Under vibrational strong coupling, an enhancement in the ionic conductivity of Cs ions was observed.

Notably, the enhancement of ionic conductivity for Cs^+, Rb^+, and K^+ ions exceeded that predicted by the limit of the Hubbard–Onsager model.[52,53] The enhancement of ionic conductivity gradually decreased with increasing the ionic radius. The observed changes in ionic conductivity under vibrational strong coupling suggest the existence of a novel mechanism to accelerate the rate of the response of hydration under vibrational strong coupling.

Finally, we discuss the effect of thermodynamic parameters on the changes in ionic conductivity under vibrational strong coupling. Fig. 5 illustrates the correlation between thermodynamic parameters reported in the literature[54,55] and the observed changes in ionic conductivity and activation energy. The changes in ionic conductivity correlate with the hydration entropies. The hydration entropy is associated with the solvation of ions from the gas phase and alterations in hydrogen-bonding networks. The modification of the hydrogen-bonding network within the dynamic hydration environment plays a crucial role in increasing the ionic conductivity by modifying the dielectric friction. Furthermore, the hydration enthalpy can be linked to the mechanism responsible for the change in ionic conduction. For bulk systems, the activation energies are independent of the ionic species according to the vehicle mechanism. This is usually explained by the competition between viscosity and migration effects in ion conduction. Under the conditions of vibrational strong coupling, the hydrogen-bonding network can be modified, even in the absence of light. This is reminiscent with the recent demonstration on the modification of the solvent polarity with the dispersion force.[31] The coherent interaction of the hydrogen-bonding environment in the water cavity can lead to the modification of the dynamic hydration network.

The chemical phenomena under vibrational strong coupling are still largely unexplored across various research fields.[24] Very recently, theoretical calculations have suggested that the dissociation rate of water molecules can be accelerated under vibrational strong coupling.[56] This theoretical study supports our conclusion that intermolecular hydrogen-bonding dynamics can be modified under vibrational strong coupling. Further advanced models could be needed to explain thermodynamics and kinetics of the system in detail. As for kinetics, our systematic study has revealed the potential for modifying the transport number in ionic conduction through dynamic hydration modifications. Moreover, it demonstrates the

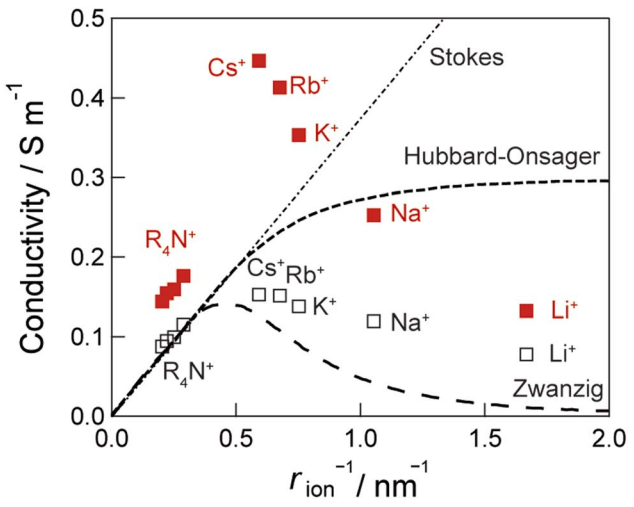

Fig. 4 Ionic radius as a function of ionic conductivity. The values for LiCl, NaCl, KCl, RbCl, CsCl, and tetraalkyl ammonium electrolyte solutions with the cavity under vibrational strong coupling (closed red symbols) without the cavity (open black symbols) were plotted. The dotted lines represent the Zwanzig model[50,51] and Hubbard–Onsager model.[52,53]

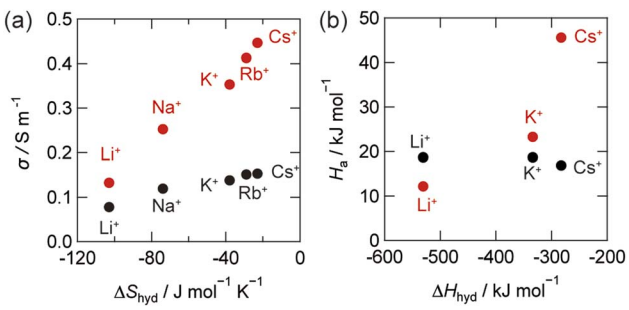

Fig. 5 (a) Correlation of hydration entropies and the ionic conductivity in the cavity, σ_{cav}, and bulk, σ_{bulk}. (b) Correlation of the hydration enthalpy and activation energies of σ_{cav} (red) and σ_{bulk} (black). The hydration enthalpy values[53] and hydration entropy values[54] were taken from the literature.

possibility of using vibrational polaritons for further exploration in the field of electrochemical energy conversion, which is based on the properties of water.[8,9]

Conclusions

In conclusion, we have demonstrated the potential of vibrational strong coupling to modify ionic conductivities. The observed modifications in ionic conductivity were found to depend on the ion radius. This is derived from the nature of hydration from structure-breaking to structure-making. The formation of polaritons effectively modified the dynamic, collective, and coherent hydration network, resulting in significant enhancements in ionic conductivity. In addition, we proposed that the entropic term in hydration plays a role in the modulation of ionic conductivity. The use of polaritons opens up new possibilities for exploring the chemical space and designing innovative materials.

Data availability

The experimental details and datasets supporting this article are available in the ESI.†

Author contributions

T. F. and K. M. conceived the project. T. F. and S. Y. designed the experiments. S. Y. and T. F. performed the experiments. All authors discussed the results and commented on the manuscript.

Conflicts of interest

There are no conflicts to declare.

Acknowledgements

This work was supported by JSPS KAKENHI (grant numbers JP21K14596, JP 22H02023, and JP22K18315). Supports by the JST-Mirai Program (JPMJMI21EB), the Photo-excitonix Project at Hokkaido University, and the MEXT Program: Data Creation and Utilization-Type Material Research and Development Project (JPMXP1122712807) are also acknowledged.

Notes and references

1 K.-D. Kreuer, Proton Conductivity: Materials and Applications, *Chem. Mater.*, 1996, **8**, 610–641.
2 K. D. Kreuer, Proton-Conducting Oxides, *Annu. Rev. Mater. Res.*, 2003, **33**, 333–359.
3 S. Horike, D. Umeyama and S. Kitagawa, Ion conductivity and transport by porous coordination polymers and metal-organic frameworks, *Acc. Chem. Res.*, 2013, **46**, 2376–2384.
4 N. Masuda, Y. Kobayashi, O. Hernandez, T. Bataille, S. Paofai, H. Suzuki, C. Ritter, N. Ichijo, Y. Noda, K. Takegoshi, C. Tassel, T. Yamamoto and H. Kageyama, Hydride in $BaTiO_{2.5}H_{0.5}$: A Labile Ligand in Solid State Chemistry, *J. Am. Chem. Soc.*, 2015, **137**, 15315–15321.
5 D. Chao, W. Zhou, F. Xie, C. Ye, H. Li, M. Jaroniec and S. Z. Qiao, Roadmap for advanced aqueous batteries: from design of materials to applications, *Sci. Adv.*, 2020, **6**, eaba4098.
6 Y. H. Wang, S. Zheng, W. M. Yang, R. Y. Zhou, Q. F. He, P. Radjenovic, J. C. Dong, S. Li, J. Zheng, Z. L. Yang, G. Attard, F. Pan, Z. Q. Tian and J. F. Li, In situ Raman spectroscopy reveals the structure and dissociation of interfacial water, *Nature*, 2021, **600**, 81–85.
7 R. E. Warburton, A. V. Soudackov and S. Hammes-Schiffer, Theoretical Modeling of Electrochemical Proton-Coupled Electron Transfer, *Chem. Rev.*, 2022, **122**, 10599–10650.
8 J. O. M. Bockris, A. K. N. Reddy, M. Gamboa-Aldeco, *Volume 2: Modern Electrochemistry: Fundamentals of Ecectrodics*, 1998.
9 J. O. M. Bockris and A. K. N. Reddy, *Volume 1: Modern Electrochemistry: Ionics*, 1998.
10 H. Ohtaki and T. Radnai, Structure and dynamics of hydrated ions, *Chem. Rev.*, 2002, **93**, 1157–1204.
11 Y. Marcus, Effect of ions on the structure of water: structure making and breaking, *Chem. Rev.*, 2009, **109**, 1346–1370.
12 M. Eigen, Proton Transfer, Acid-Base Catalysis, and Enzymatic Hydrolysis. Part I: Elementary Processes, *Angew. Chem., Int. Ed.*, 1964, **3**, 1–19.
13 P. G. Wolynes, Dynamics of Electrolyte Solutions, *Annu. Rev. Phys. Chem.*, 1980, **31**, 345–376.
14 D. Marx, M. E. Tuckerman, J. Hutter and M. Parrinello, The nature of the hydrated excess proton in water, *Nature*, 1999, **397**, 601–604.
15 P. L. Geissler, C. Dellago, D. Chandler, J. Hutter and M. Parrinello, Autoionization in liquid water, *Science*, 2001, **291**, 2121–2124.
16 M. E. Tuckerman, D. Marx and M. Parrinello, The nature and transport mechanism of hydrated hydroxide ions in aqueous solution, *Nature*, 2002, **417**, 925–929.
17 B. E. Conway, J. O. Bockris and H. Linton, Proton Conductance and the Existence of the H_3O^+ Ion, *J. Chem. Phys.*, 1956, **24**, 834–850.
18 B. E. Conway and J. O. M. Bockris, Proton Conductance in Ice, *J. Chem. Phys.*, 1958, **28**, 354–355.
19 K. D. Kreuer, On the complexity of proton conduction phenomena, *Solid State Ionics*, 2000, **136**, 149–160.
20 N. Agmon, The Grotthuss mechanism, *Chem. Phys. Lett.*, 1995, **244**, 456–462.
21 C. J. T. Grotthuss, Sur la décomposition de l'eau et des corps q'uelle tient en dissolution à l'aide de l'électricité galvanique, *Ann. Chim.*, 1806, **LVIII**, 54–74.
22 K.-D. Kreuer, A. Rabenau and W. Weppner, Vehicle Mechanism, a New Model for the Interpretation of the Conductivity of Fast Proton Conductors, *Angew Chem. Int. Ed. Engl.*, 1982, **21**, 208–209.
23 R. Biswas and B. Bagchi, Limiting Ionic Conductance of Symmetrical, Rigid Ions in Aqueous Solutions: Temperature Dependence and Solvent Isotope Effects, *J. Am. Chem. Soc.*, 1997, **119**, 5946–5953.

24 K. Nagarajan, A. Thomas and T. W. Ebbesen, Chemistry under Vibrational Strong Coupling, *J. Am. Chem. Soc.*, 2021, **143**, 16877–16889.
25 F. J. Garcia-Vidal, C. Ciuti and T. W. Ebbesen, Manipulating matter by strong coupling to vacuum fields, *Science*, 2021, **373**, eabd0336.
26 T. W. Ebbesen, Hybrid Light-Matter States in a Molecular and Material Science Perspective, *Acc. Chem. Res.*, 2016, **49**, 2403–2412.
27 B. S. Simpkins, A. D. Dunkelberger and J. C. Owrutsky, Mode-Specific Chemistry through Vibrational Strong Coupling (or A Wish Come True), *J. Phys. Chem. C*, 2021, **125**, 19081–19087.
28 J. P. Long and B. S. Simpkins, Coherent Coupling between a Molecular Vibration and Fabry–Perot Optical Cavity to Give Hybridized States in the Strong Coupling Limit, *ACS Photonics*, 2014, **2**, 130–136.
29 A. Shalabney, J. George, J. Hutchison, G. Pupillo, C. Genet and T. W. Ebbesen, Coherent coupling of molecular resonators with a microcavity mode, *Nat. Commun.*, 2015, **6**, 5981.
30 T. E. Li, A. Nitzan and J. E. Subotnik, On the origin of ground-state vacuum-field catalysis: equilibrium consideration, *J. Chem. Phys.*, 2020, **152**, 234107.
31 M. Piejko, B. Patrahau, K. Joseph, C. Muller, E. Devaux, T. W. Ebbesen and J. Moran, Solvent Polarity under Vibrational Strong Coupling, *J. Am. Chem. Soc.*, 2023, **145**(24), 13215–13222.
32 T. Fukushima, S. Yoshimitsu and K. Murakoshi, Vibrational Coupling of Water from Weak to Ultrastrong Coupling Regime via Cavity Mode Tuning, *J. Phys. Chem. C*, 2021, **125**, 25832–25840.
33 R. M. A. Vergauwe, A. Thomas, K. Nagarajan, A. Shalabney, J. George, T. Chervy, M. Seidel, E. Devaux, V. Torbeev and T. W. Ebbesen, Modification of Enzyme Activity by Vibrational Strong Coupling of Water, *Angew. Chem., Int. Ed.*, 2019, **58**, 15324–15328.
34 J. Lather and J. George, Improving Enzyme Catalytic Efficiency by Co-operative Vibrational Strong Coupling of Water, *J. Phys. Chem. Lett.*, 2021, **12**, 379–384.
35 K. Gu, Q. Si, N. Li, F. Gao, L. Wang and F. Zhang, Regulation of Recombinase Polymerase Amplification by Vibrational Strong Coupling of Water, *ACS Photonics*, 2023, **10**, 1633–1637.
36 C. Zhong, S. Hou, X. Zhao, J. Bai, Z. Wang, F. Gao, J. Guo and F. Zhang, Driving DNA Origami Coassembling by Vibrational Strong Coupling in the Dark, *ACS Photonics*, 2023, **10**, 1618–1623.
37 K. Hirai, H. Ishikawa, T. Chervy, J. A. Hutchison and I. H. Uji, Selective crystallization via vibrational strong coupling, *Chem. Sci.*, 2021, **12**, 11986–11994.
38 T. Fukushima, S. Yoshimitsu and K. Murakoshi, Inherent Promotion of Ionic Conductivity via Collective Vibrational Strong Coupling of Water with the Vacuum Electromagnetic Field, *J. Am. Chem. Soc.*, 2022, **144**, 12177–12183.
39 G. Khitrova, H. M. Gibbs, M. Kira, S. W. Koch and A. Scherer, Vacuum Rabi splitting in semiconductors, *Nat. Phys.*, 2006, **2**, 81–90.
40 P. Torma and W. L. Barnes, Strong coupling between surface plasmon polaritons and emitters: a review, *Rep. Prog. Phys.*, 2015, **78**, 013901.
41 J. Stenger, D. Madsen, P. Hamm, E. T. J. Nibbering and T. Elsaesser, Ultrafast Vibrational Dephasing of Liquid Water, *Phys. Rev. Lett.*, 2001, **87**, 027401.
42 A. Kadyan, A. Shaji and J. George, Boosting Self-interaction of Molecular Vibrations under Ultrastrong Coupling Condition, *J. Phys. Chem. Lett.*, 2021, **12**, 4313–4318.
43 J. George, T. Chervy, A. Shalabney, E. Devaux, H. Hiura, C. Genet and T. W. Ebbesen, Multiple Rabi Splittings under Ultrastrong Vibrational Coupling, *Phys. Rev. Lett.*, 2016, **117**, 153601.
44 R. H. Boyd, Extension of Stokes' Law for Ionic Motion to Include the Effect of Dielectric Relaxation, *J. Chem. Phys.*, 1961, **35**, 1281–1283.
45 A. L. Levy, Ionic Hydration and Stokes' Law, *J. Chem. Phys.*, 1953, **21**, 566–567.
46 L. J. Gagliardi, Dielectric friction and protonic mobility, *J. Chem. Phys.*, 1973, **58**, 2193–2194.
47 L. J. Gagliardi, Protonic mobility and hydration, *J. Chem. Phys.*, 1974, **61**, 5465–5466.
48 M. Born, Über die Beweglichkeit der elektrolytischen Ionen, *Z. Phys.*, 1920, **1**, 221–249.
49 R. M. Fuoss, Dependence of the Walden Product on Dielectric Constant, *Proc. Natl. Acad. Sci. U. S. A.*, 1959, **45**, 807–813.
50 R. Zwanzig, Dielectric Friction on a Moving Ion, *J. Chem. Phys.*, 1963, **38**, 1603–1605.
51 R. Zwanzig, Dielectric Friction on a Moving Ion. II. Revised Theory, *J. Chem. Phys.*, 1970, **52**, 3625–3628.
52 J. Hubbard and L. Onsager, Dielectric dispersion and dielectric friction in electrolyte solutions. I, *J. Chem. Phys.*, 1977, **67**, 4850–4857.
53 J. B. Hubbard, Dielectric dispersion and dielectric friction in electrolyte solutions. II, *J. Chem. Phys.*, 1978, **68**, 1649–1664.
54 Y. Marcus, The hydration entropies of ions and their effects on the structure of water, *J. Chem. Soc., Faraday Trans. 1*, 1986, **82**, 233–242.
55 Y. Marcus, The thermodynamics of solvation of ions. Part 2—the enthalpy of hydration at 298.15 K, *J. Chem. Soc., Faraday Trans. 1*, 1987, **83**, 339–349.
56 Q. Yu and J. M. Bowman, Manipulating hydrogen bond dissociation rates and mechanisms in water dimer through vibrational strong coupling, *Nat. Commun.*, 2023, **14**, 3527.